

Thermoelectric response in two-dimensional Dirac systems: Role of particle-hole pairs

Kitinan Pongsangangan, Simonas Grubinskas, and Lars Fritz 

Institute for Theoretical Physics, Utrecht University, 3584 CE Utrecht, Netherlands

 (Received 15 May 2022; revised 25 August 2022; accepted 11 October 2022; published 15 November 2022)

Clean two-dimensional Dirac systems have received a great deal of attention for being a prime candidate to observe hydrodynamical transport behavior in interacting electronic systems. This is mostly due to recent advances in the preparation of ultrapure samples with sufficiently strong interactions. In this paper we investigate the role of collective modes in the thermoelectric transport properties of those systems. We find that dynamical particle-hole pairs, plasmons, make a sizable contribution to the thermal conductivity. While the increase at the Dirac point is moderate, it becomes large towards larger doping. We suspect that this is a generic feature of ultraclean two-dimensional electronic systems, also applicable to degenerate systems.

DOI: [10.1103/PhysRevResearch.4.043107](https://doi.org/10.1103/PhysRevResearch.4.043107)

I. INTRODUCTION

The study of transport in metallic systems has a long and successful history, going back all the way to Drude transport theory [1]. Remarkably, a picture of noninteracting electrons scattering from disorder provides a reasonable description of transport properties of metals or more specifically Fermi liquids. In general, however, electrons are interacting and a question that has been discussed for 70 years is why the picture of independent electrons diffusing in a disordered background is so successful [2]. To rephrase the question, why and how do the long-range correlations between electrons due to Coulomb interaction become ineffective? Bohm and Pines argued that there are two components associated with the Coulomb interaction, short- and long-range parts, and they play very different roles. The short-range part leads to a quasiparticle renormalization in the spirit of Landau's Fermi liquid theory, leading to "new" almost free electrons. The primary manifestation of the long-range part is the plasma oscillations or plasmons [3,4]. In the standard theory of metallic transport, interactions consequently play a minor role in the low-temperature limit. There are two ways in which they enter: (i) as a source of inelastic scattering for the electronic quasiparticles [5] and (ii) as dynamical collective degrees of freedom like plasmons that make a direct contribution to transport properties. In conventional three-dimensional Fermi liquids, neither of the two happens. (i) Inelastic scattering is subdominant compared to elastic impurity scattering. It is parametrically small in $(T/T_F)^2$, where $T_F \approx 10^3\text{--}10^5$ K is the Fermi temperature of the metallic system. (ii) In a three-dimensional metal, stable plasmons are gapped, showing a gap that is even larger than the Fermi energy of the electronic

system. This implies that they cannot be excited at energy scales relevant for transport [6,7]. As a consequence, only electrons are relevant in the low-energy limit and they interact with each other through the residual short-range component of the interaction. The primary source of scattering is given by disorder (note that we do not consider the role of phonons throughout this work [8]). One of the consequences of this is the famous Wiedemann-Franz law, which goes back to 1853 [9]. It states that at lowest temperatures in metals the ratio

$$\lim_{T \rightarrow 0} \frac{\kappa}{T\sigma} = L_0 \quad (1)$$

is constant and independent of details of the system. In Eq. (1) T is the temperature, σ is the electrical conductivity, κ is the heat conductivity, and $L_0 = (\pi^2/3)/(k_B/e)^2$ is the Lorenz number (k_B is the Boltzmann constant and e the electron charge). One way to rationalize this finding is that at the lowest energies only electrons carry charge and heat and both transport channels undergo the same scattering mechanisms from disorder. This leads to the same scattering time for both charge and heat transport. The question whether inelastic scattering can be the dominant scattering mechanism in degenerate Fermi systems was discussed in the 1960s [10,11] but recently gained more momentum [12–14]. The general expectation is that one should then observe hydrodynamic transport phenomena.

Other variants of conducting and interacting electronic systems are Dirac and Weyl metals [15]. Their defining feature is a linear band crossing in isolated points in the Brillouin zone which strongly suppresses the density of states. These systems are semimetals or nondegenerate. The most famous example is graphene, which has been at the forefront of research for almost two decades [16,17].

Close to its Dirac point, pristine graphene has properties that are distinct from normal Fermi liquids. One major difference is that at the Dirac point the system is scale-free, resembling a quantum critical system [18]. Consequently, temperature T is the only energy scale, contrary to a degenerate fermionic system which possesses the Fermi temperature

Published by the American Physical Society under the terms of the Creative Commons Attribution 4.0 International license. Further distribution of this work must maintain attribution to the author(s) and the published article's title, journal citation, and DOI.

T_F . While this modifies thermodynamic properties, it also has consequences on the interaction properties: Inelastic interaction scattering cannot be suppressed by the smallness of T/T_F (also in the vicinity of the Dirac point T/T_F remains large); it can even dominate elastic scattering from disorder. Therefore, in sufficiently clean samples, it is theoretically expected that one finds hydrodynamic transport behavior [19–25]. In addition, it is known that decreasing dimensionality increases the effect of long-range interactions in electronic systems. That not only increases inelastic scattering, it also makes the effect of collective modes more prominent. It is known that plasmons in a one-dimensional conductor contribute significantly to thermal transport. This begs the question about two dimensions. In two dimensions, contrary to three dimensions, plasmons are massless [26,27] and follow a square root dispersion, i.e., $\omega \propto \sqrt{q}$. Consequently, they are easily excited under nonequilibrium conditions and can therefore be relevant to the transport phenomena, especially thermal transport. It is important to note that the second point is not exclusive to Dirac systems but is also true for two-dimensional degenerate systems.

In recent years, suspended samples or samples sandwiched in between boron-nitride structures [28–33] have allowed the suppression of disorder levels sufficiently to access the hydrodynamic regime. With the new ultrapure samples, it is thus possible to ask quantitative questions that could not be addressed before. In this paper we reinvestigate thermoelectric transport theory in ultraclean Dirac systems. Our special focus is on the role of Coulomb interactions and their unscreened long-range nature in thermoelectric transport.

As explained above, we expect the Coulomb interaction to be responsible for mainly two effects in regard to transport phenomena: (i) Charge carriers scatter from each other leading to an effective inelastic transport time or mean free path and (ii) collective excitations, such as plasmons, that possess their own dynamics. Consequently, they make a direct contribution to the heat current.

The thermoelectric response involves two types of currents: the electrical current J^e and the heat current $Q = J^E - \mu/eJ^e$, where J^E is the energy current. The Onsager relation states that [34]

$$\begin{pmatrix} \bar{J}^e \\ \bar{Q} \end{pmatrix} = \begin{pmatrix} \hat{\sigma} & \hat{\alpha} \\ T\hat{\alpha} & \hat{\kappa} \end{pmatrix} \begin{pmatrix} \vec{E} \\ -\vec{\nabla}T \end{pmatrix}. \quad (2)$$

The thermal conductivity $\hat{\kappa}$ is defined as the heat current response to a thermal gradient $-\vec{\nabla}T$ in the absence of an electrical current (electrically isolated boundaries), given by $\hat{\kappa} = \hat{\kappa} - T\hat{\alpha}\hat{\sigma}^{-1}\hat{\alpha}$. In the following we drop the circumflex and explicitly discuss only the diagonal response σ and κ . The Wiedemann-Franz ratio $\kappa/T\sigma$ assumes the value $L_0 = (\pi^2/3)(k_B/e)^2$ (L_0 is the Lorenz number) in a Fermi liquid [9] [see Eq. (1)]. This is sometimes considered the hallmark of a Fermi liquid and it was argued before that it breaks down in the vicinity of the Dirac point [22,23,30,35]. The main reason for this breakdown is that there are two completely independent hydrodynamic modes that are subject to different scattering mechanisms. Instead of concentrating on two types of degrees of freedom, electrons and holes, we additionally consider plasmons. The situations are sketched in Fig. 1 for

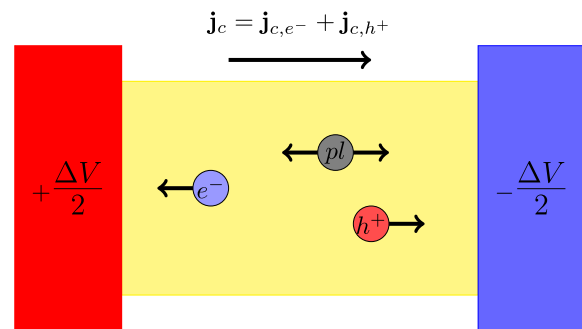


FIG. 1. Electrons and holes react oppositely to an applied voltage drop. Plasmons do not couple directly to the voltage difference; however, they experience drag and serve as a source of inelastic scattering.

electrical transport and in Fig. 2 for heat transport. The potential drop in Fig. 1 acts on electrons and holes oppositely, but not on the plasmons: The plasmons experience no direct force, but they are subject to drag effects. Being neutral quasiparticles, they do not contribute to the charge current. In the case of a temperature gradient (see Fig. 2), all particles experience a force in the same direction and there is an additional direct contribution to the current through the plasmons. On a technical level, we derive and solve three coupled Boltzmann equations for electrons, holes, and plasmons, which include relaxational processes and the respective streaming terms.

Main result. We find that the plasmon contribution to the heat conductivity is sizable and cannot be neglected either at the Dirac point or in the degenerate limit.

II. MODEL

We study a model of Dirac fermions coupled through Coulomb interaction and subject to potential disorder

$$\begin{aligned} H = & \int d^2\vec{r} \Psi_i^\dagger(\vec{r}) [-iv_F \vec{\partial} \cdot \vec{\sigma} + V_{\text{dis}}(\vec{r})] \Psi_i(\vec{r}) \\ & + \frac{1}{2} \int d^2\vec{r} d^2\vec{r}' \Psi_i^\dagger(\vec{r}) \Psi_i(\vec{r}) V(\vec{r} - \vec{r}') \Psi_j^\dagger(\vec{r}') \Psi_j(\vec{r}'), \end{aligned} \quad (3)$$

where $\Psi_i(\vec{r})$ is the two-component wave function, i is the flavor index in the range $i = 1, \dots, N$ (for graphene $N =$

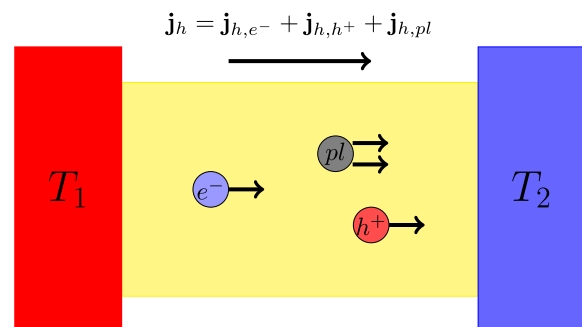


FIG. 2. Electrons, holes, and plasmons react to a temperature gradient in the same manner. Plasmons make a direct contribution to the heat current.

4 counting spin and valley), v_F is the Fermi velocity, and $V(\vec{r} - \vec{r}') = \alpha \frac{v_F}{|\vec{r} - \vec{r}'|}$ is the Coulomb interaction (note that double indices are summed over). The dimensionless fine-structure constant sets the strength of interaction and is given by $\alpha = e^2/4\pi\epsilon_0\epsilon_r v_F$. The disorder potential $V_{\text{dis}}(\vec{r})$ can be used to describe a variety of disorder types specified by the disorder correlation function. We only consider δ -correlated disorder, i.e., $\langle V_{\text{dis}}(\vec{r})V_{\text{dis}}(\vec{r}') \rangle = 4\pi\gamma^2\delta(\vec{r} - \vec{r}')$, but generalizations are straightforward. Consequently, the parameters of our theory are α and γ . Equation (3) does not provide a convenient starting point for the study of the thermal conductivity due to the nonlocal Coulomb interaction.

A corresponding local field theory that easily lends itself to an interpretation in terms of plasmons can be derived using a Hubbard-Stratonovich transformation. It reads

$$\begin{aligned} \mathcal{L} = & -\frac{\epsilon_0\epsilon_r}{2}\phi(\vec{r}, z, t)(\vec{\partial}^2 + \partial_z^2)\phi(\vec{r}, z, t) \\ & - e\Psi_\alpha^\dagger(\vec{r}, t)\Psi_\alpha(\vec{r}, t)\phi(\vec{r}, z, t)\delta(z) \\ & + \Psi_\alpha^\dagger(\vec{r}, t)[i\partial_t - iv_F\vec{\partial} \cdot \vec{\sigma} + V_{\text{dis}}(\vec{r})]\delta(z)\Psi_\alpha(\vec{r}, t), \end{aligned} \quad (4)$$

where $\phi(\vec{r}, z, t)$ is the real-valued plasmon field. Importantly, the mapping between Eqs. (3) and (4) is exact.

A. Current operators

The electrical charge current is only carried by electrons and holes and its density is given by

$$\mathbf{j}^e(\vec{r}, t) = -ev_F\Psi_\alpha^\dagger(\vec{r}, t)\vec{\sigma}\Psi_\alpha(\vec{r}, t). \quad (5)$$

The heat current density is given by $\mathbf{Q} = \mathbf{j}^E - \mu/e\mathbf{j}^e$, where the energy current density reads

$$\begin{aligned} \mathbf{j}^E(\vec{r}, z, t) = & -iv_F\Psi_\alpha^\dagger(\vec{r}, t)\vec{\sigma}\partial_t\Psi_\alpha(\vec{r}, t) \\ & + \epsilon_0\epsilon_r\vec{\partial}\phi(\vec{r}, z, t)\partial_t\phi(\vec{r}, z, t). \end{aligned} \quad (6)$$

This expression explicitly includes the plasmon contribution, which is the main different aspect of this work.

B. Plasmon dynamics

Integrating out the photon modes outside the graphene sheet leads to an effective two-dimensional theory $\mathcal{S}_\Phi = \frac{1}{2} \int dt d\vec{r} d^2\vec{r}' \Phi(\vec{r}, t)D_0^{-1}(\vec{r}, \vec{r}', t, t')\Phi(\vec{r}', t')$ with $\Phi(\vec{r}, t) = \phi(\vec{r}, z=0, t)$ and $D_0^{-1}(\vec{k}, \omega) = \alpha(2\pi v_F)/e^2k$ with $k = |\vec{k}|$. The dynamics is generated from within the fermionic system and corresponds to particle-hole pairs. We use the standard random-phase approximation (RPA), formally justified in the limit of a large number N of flavors. The boson self-energy is approximated through $e^2\Pi(\vec{r}, \vec{r}', t, t')$, where $\Pi(\vec{r}, \vec{r}', t, t')$ is the polarization function. The polarization function of two-dimensional Dirac systems has a closed analytical form at zero temperature [26]. The finite-temperature properties at arbitrary chemical potential were studied numerically in Ref. [27]. In the long-wavelength limit, important for the plasmon dynamics, the retarded polarization function can be approximated as

$$\begin{aligned} \Pi^r(\vec{q}, \omega, \mu, T) \approx & \frac{Nq^2T}{4\pi\omega^2} \ln\left[2 + 2\cosh\left(\frac{\mu}{T}\right)\right] \\ & - i\frac{Nq^2}{32\omega}f(\mu, \omega, T), \end{aligned} \quad (7)$$

with $f(\mu, \omega, T) = \tanh(\frac{\mu}{2T} - \frac{\omega}{4T}) - \tanh(\frac{\mu}{2T} + \frac{\omega}{4T})$. We obtain the plasmon dispersion from the poles of the retarded plasmon propagator

$$D^r(\vec{q}, \omega) = \frac{D_0^r(\vec{q}, \omega)}{1 - e^2D_0^r(\vec{q}, \omega)\Pi^r(\vec{q}, \omega, \mu, T)}, \quad (8)$$

where $D_0^r(\vec{q}, \omega) = 1/2\epsilon_0\epsilon_r q$, with ϵ_0 the vacuum permittivity and ϵ_r the relative permittivity. Using the approximate polarization function (7), we can approximate the plasmon propagator as

$$D^r(\vec{q}, \omega) \approx \frac{1}{2\epsilon_0\epsilon_r} \frac{\omega^2}{q} \frac{1}{(\omega + i0^+)^2 - [\omega_p(\vec{q}) + i\gamma_p(\vec{q})]^2}, \quad (9)$$

with the plasmon dispersion $\omega_p(\vec{q})$ and damping $\gamma_p(\vec{q})$ given by

$$\begin{aligned} \omega_p(\vec{q}) = & \sqrt{\alpha \frac{N}{2} k_B T v_F q \ln\left[2 + 2\cosh\left(\frac{\mu}{k_B T}\right)\right]}, \\ \gamma_p(\vec{q}) = & -\frac{\pi\omega_p(\vec{q})^2}{16T} \frac{f(\mu, \omega_p(\vec{q}), T)}{\ln[2 + 2\cosh(\frac{\mu}{T})]}. \end{aligned} \quad (10)$$

There are two possible momentum cutoffs for the plasmons of Eq. (10): either when they cease to be well-defined quasiparticles, i.e., $\omega_p(\vec{q}_c) \approx \gamma_p(\vec{q}_c)$, or when the square-root dispersion breaks down, i.e., $q_c = \alpha NT/2v_F \ln[2 + 2\cosh(\mu/T)]$. Numerically, we always choose the lower of the two. In practice, it turns out that it is always the latter. For all practical calculations in this paper, we assume the plasmons to be well-defined quasiparticles with the reasoning given above. It turns out that below q_c plasmons are very stable against a single particle-hole decay channel. Therefore, the leading relaxation mechanisms might be from either the plasmon decay into two electron-hole pairs [36] or phonon-assisted Landau damping [37]. Both are neglected in this work for different reasons. The former channel is of higher order in perturbation theory and beyond the RPA, while the latter is forbidden in the electron hydrodynamic window. It will however become important at higher densities, which is left for future studies. It is important to note that there is also a linear plasmon beyond the cutoff scale which is subleading and consequently negligible in our analysis.

C. Boltzmann equation

We leave a systematic derivation of the Boltzmann equation starting from the Schwinger-Keldysh formalism (see, for instance, Ref. [38]) for Appendices A–D. The key steps of the derivation are (i) a conserving approximation of the fermion and boson self-energies to the lowest nontrivial order in α and γ , (ii) a lowest nontrivial order gradient expansion starting from the Wigner transform, (iii) an integration over the fermion and boson spectral functions, equivalent to an on-shell quasiparticle approximation, and (iv) a projection into the quasiparticle basis. In the last step we consider only the diagonal parts and neglect Berry phase (these terms are second order in the gradient expansion) and zitterbewegung terms (see Ref. [20,21]). Eventually, we find three coupled Boltzmann equations for electrons, holes, and

plasmons,

$$\begin{aligned} e\vec{E}\partial_{\vec{k}}f_{\lambda}(\vec{k}) - \lambda v_F \hat{k}\sigma_z \vec{\nabla}T \partial_T f_{\lambda}(\vec{k}) &= I_{\text{coll}}^{\lambda}[f_{\lambda}, b], \\ 2\frac{\vec{k}}{k^2}\vec{\nabla}T\omega_p(\vec{k})\partial_T b_{\omega_p(\vec{k})}(\vec{k}) &= \tilde{I}_{\text{coll}}[f_{\lambda}, b]. \end{aligned} \quad (11)$$

Here f_{λ} and b are the distribution functions of the electrons and holes ($\lambda = \pm$) and the plasmons, respectively.

D. Sources of current relaxation

The collision integral for the Dirac fermions consists of two independent parts

$$\begin{aligned} I_{\text{coll}}^{\lambda} &= \int \frac{d^2q}{(2\pi)^2} \sum_{\lambda'=\pm} C_{\lambda\lambda'}^{\text{inel}}(\vec{k}, \vec{q}) \{f_{\lambda}(\vec{k})[1 - f_{\lambda'}(\vec{k} + \vec{q})] \\ &\quad - b_{\epsilon_{\lambda}(\vec{k}) - \epsilon_{\lambda'}(\vec{k} + \vec{q})}(\vec{q})[f_{\lambda'}(\vec{k} + \vec{q}) - f_{\lambda}(\vec{k})]\} \\ &\quad + \int \frac{d^2q}{(2\pi)^2} C_{\lambda}^{\text{el}}(\vec{k}, \vec{q}) [f_{\lambda}(\vec{k}) - f_{\lambda}(\vec{k} + \vec{q})]. \end{aligned} \quad (12)$$

The first term accounts for inelastic scattering of electrons from plasmons, denoted by $C_{\lambda\lambda'}^{\text{inel}}$. In this process, both energy and momentum are transferred between the fermions and the plasmons. Additionally, there is elastic scattering from disorder, encoded in C_{λ}^{el} . This term breaks momentum conservation and is important to relax the heat current. The collision integral for the plasmons reads

$$\begin{aligned} \tilde{I}_{\text{coll}} &= \int \frac{d^2q}{(2\pi)^2} \sum_{\lambda, \lambda'=\pm} \tilde{C}_{\lambda\lambda'}^{\text{inel}} \{f_{\lambda'}(\vec{k} + \vec{q})[f_{\lambda}(\vec{q}) - 1] \\ &\quad - b_{\epsilon_{\lambda'}(\vec{k} + \vec{q}) - \epsilon_{\lambda}(\vec{q})}(\vec{k})[f_{\lambda'}(\vec{k} + \vec{q}) - f_{\lambda}(\vec{q})]\}. \end{aligned} \quad (13)$$

It contains an inelastic part describing scattering from fermions, $\tilde{C}_{\lambda\lambda'}^{\text{inel}}$ (the role of inelastic scattering from disorder is beyond the scope of the present work). In the absence of disorder, the combined electron-plasmon system conserves momentum. The precise form of $C_{\lambda\lambda'}^{\text{inel}}$, C_{λ}^{el} , and $\tilde{C}_{\lambda\lambda'}^{\text{inel}}$ can be found in Appendix D. It is important to note, however, that momentum excited in the plasmon sector can be relaxed in the fermion sector from disorder.

E. Linearized Boltzmann equation

In equilibrium, the collision integrals are nullified by the thermal Fermi-Dirac and Bose-Einstein distributions $f_{\lambda}^0(\vec{k}) = (e^{(\epsilon_{\lambda}(\vec{k}) - \mu)/T} + 1)^{-1}$ and $b_{\omega}^0(\vec{k}) = (e^{\omega_p(\vec{k})/T} - 1)^{-1}$, respectively. In the presence of driving terms due to a potential gradient or a thermal gradient or both, the distribution functions deviate from their equilibrium form. Importantly, even though an electric field does not couple directly to the plasmons, away from the Dirac point they are still driven out of equilibrium by a drag effect.¹ Since we are interested in linear response transport properties, we linearize the Boltzmann equations in \vec{E} and $\vec{\nabla}T$. This enforces the following

parametrizations for the fermions and boson distribution functions:

$$\begin{aligned} f_{\lambda}(\vec{k}) &= f_{\lambda}^0(\vec{k}) + 1/T^2 f_{\lambda}^0(\vec{k})[1 - f_{\lambda}^0(\vec{k})]\lambda v_F \hat{k} \\ &\quad \cdot [e\vec{E}\chi_{\lambda}^E(k) + \vec{\nabla}T\chi_{\lambda}^T(k)], \\ b_{\omega_p(\vec{k})}(\vec{k}) &= b_{\omega_p(\vec{k})}^0(\vec{k}) + 1/T^2 b_{\omega_p(\vec{k})}^0(\vec{k})[1 + b_{\omega_p(\vec{k})}^0(\vec{k})]v_F \hat{k} \\ &\quad \cdot [e\vec{E}\phi^E(k) + \vec{\nabla}T\phi^T(k)]. \end{aligned} \quad (14)$$

As mentioned before, an electric field applied to the fermions “drags” the plasmons out of equilibrium, which is why we have to introduce ϕ^E . The functions $\chi_{\lambda}^{T,E}$ and $\phi^{T,E}$ have to be determined numerically and give access to the respective currents and related response functions. In terms of their parametrizations, we find the set of equations

$$\begin{aligned} -\lambda e \frac{v_F}{T} \hat{k} \cdot \vec{E} f_{\lambda}^0(\vec{k}) [1 - f_{\lambda}^0(\vec{k})] \\ - \lambda \frac{v_F}{T} \hat{k} \vec{\nabla}T \frac{\epsilon_{\lambda}(\vec{k}) - \mu}{T} f_{\lambda}^0(\vec{k}) [1 - f_{\lambda}^0(\vec{k})] \\ = I_{\text{inel}}^{\text{lin}}[\chi_T, \chi_E, \phi_T, \phi_E] + I_{\text{el}}^{\text{lin}}[\chi_E, \chi_T], \\ \frac{\vec{k}}{k^2} \vec{\nabla}T \frac{\omega_p^2(\vec{k})}{T^2} b_{\omega_p(\vec{k})}^0(\vec{k}) [1 + b_{\omega_p(\vec{k})}^0(\vec{k})] \\ = \tilde{I}_{\text{inel}}^{\text{lin}}[\chi_T, \chi_E, \phi_T, \phi_E] + \tilde{I}_{\text{inel}}^{\text{el}}[\phi_T, \phi_E], \end{aligned} \quad (15)$$

with details to be found in Appendix E. In the absence of disorder, the combined system of fermions and plasmons possesses a zero mode associated with momentum conservation, meaning the combination $C_{\lambda\lambda'}^{\text{inel}}$ and $\tilde{C}_{\lambda\lambda'}^{\text{inel}}$ together with the appropriate mode cannot relax momentum (we explicitly checked this point numerically). The intuition behind this is that momentum can always be transferred between the fermion and plasmon sector without being dissipated. This implies that disorder scattering is vital as a source of momentum relaxation for the total system and it plays an important role in the choice of modes, explained below (see Ref. [8] for a related discussion in the electron-phonon problem without umklapp scattering).

F. Choice of modes

The above parametrization allows for a very transparent identification of the slow hydrodynamic modes of the problem. In the solution of the fermion-only problem (3), it was pointed out that in order to study thermoelectric transport in the vicinity of the Dirac point all the way to the Fermi liquid regime, it suffices to study two types of modes for electrons and holes $\chi_{\lambda}^{T,E}(k) = a_{0,\lambda}^{T,E} + \lambda a_{1,\lambda}^{T,E}k$, respectively [22]. The mode associated with $a_{0,\lambda}^{T,E}$ is called the chiral mode, whereas the one associated with $a_{1,\lambda}^{T,E}$ corresponds to the momentum mode. For the plasmons, the equivalent ansatz reads $\phi^{T,E}(k) = b_0^{E,T} + b_1^{T,E}k$. We can convert the problem of solving the Boltzmann equation into a linear algebra problem by projecting the scattering integral onto the respective modes (see the discussion in Appendix E).

¹At the Dirac point the underlying particle-hole symmetry forbids drag [39].

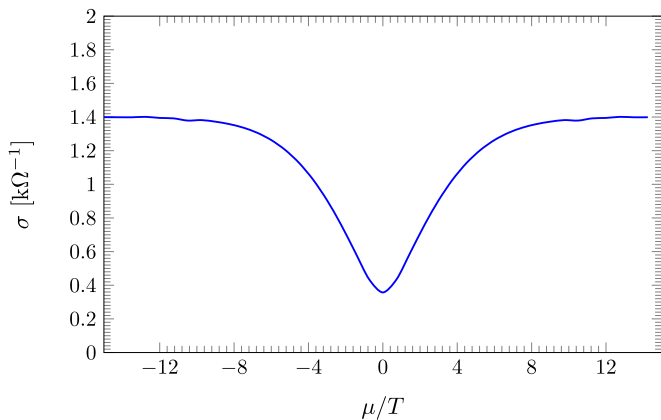


FIG. 3. Electrical conductivity as a function of chemical potential. The curve was obtained as the solution of the Boltzmann equation with $\alpha = 0.36$ and $4\pi\gamma^2 = 0.5$ at $T = 75$ K

III. RESULTS

We have solved the coupled Boltzmann equations (15) at and away from the Dirac point. This allows us to access both the electrical and the heat conductivity and consequently the Wiedemann-Franz ratio. In the following we present two types of plots: (a) the conductivities as a function of the chemical potential (Figs. 3–5) and more experimentally relevant (b) the conductivities as a function of the electronic density (Figs. 6–8). In all plots we have fixed the temperature to be $T = 75$ K and the fine-structure constant α to be $\alpha = 0.36$. For disorder, we made the assumption that it is short ranged and $4\pi\gamma^2 = 0.5$. In graphene, it is generally believed that disorder is long ranged, but here we are concerned with only a generic mechanism and aim to keep the number of parameters small. We have checked that the general conclusion does not change upon using a more realistic and complicated disorder potential. In all plots, we plot the total conductivity including the plasmon contribution in blue and the electronic contribution only in red.

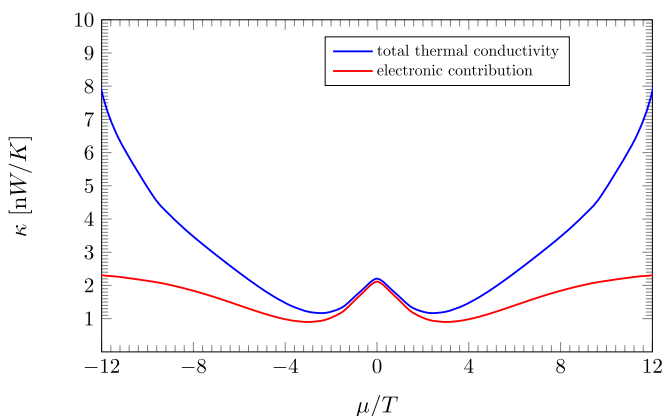


FIG. 4. Thermal conductivity of graphene as a function of the chemical potential. The curves are calculated using the same set of parameters used in Fig. 3. The blue curve is the full response including the plasmons, while the red curve only shows the electronic contribution. There is a slight plasmon enhancement close to the Dirac point and a massive one with increasing chemical potential.

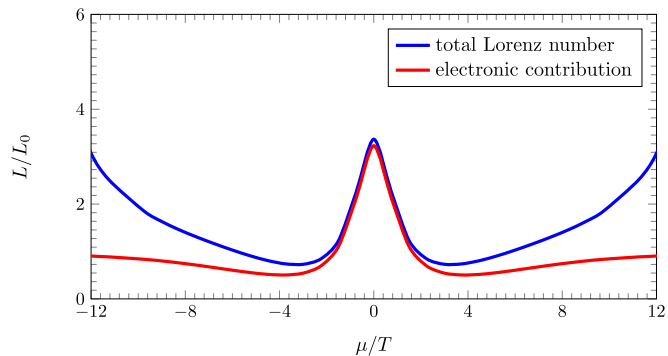


FIG. 5. Wiedemann-Franz ratio as a function of the chemical potential. We observe two regions with enhancement: the well-known hydrodynamic regime in the vicinity of the Dirac point and at higher doping.

Since the plasmons cannot make a direct contribution to the electrical conductivity, there is only a blue line in Figs. 3 and 6.

It should be mentioned that this work is consistent with the previous work by one of the authors and collaborators [21]. In [21] the electrical conductivity at the Dirac point is given by $\sigma = \frac{e^2}{h} \frac{0.76}{\alpha^2}$. The prefactor 0.76 is what the Boltzmann equation solution determines. The fine-structure constant α is renormalized as a function of temperature and follows $\alpha = \frac{\alpha_0}{1 + (\alpha_0/4) \ln(\Lambda/T)}$. For a realistic cutoff of $\Lambda = 3$ eV, the chosen value of $\alpha_0 = 0.36$ and $T = 75$ K give the renormalized fine-structure constant $\alpha \approx 0.23$ and $\sigma = 14.37e^2/h \approx 0.6$ $k\Omega^{-1}$. Additionally, there is an additional source of scattering: disorder. While this is subdominant, it still makes a correction and reduces σ approximately to 0.4 $k\Omega^{-1}$, as shown in Fig. 3.

We observe that there is an enhancement of the thermal conductivity close to the Dirac point. This enhancement increases the expected violation of the Wiedemann-Franz law at the Dirac point. A bit more surprisingly, however, there is a sizable and increasing enhancement of the thermal conductivity towards the Fermi liquid regime, i.e., $\mu \gg T$. The reason is that plasmons are more stable at higher electronic densities. This simple argument can be checked in the relaxation time

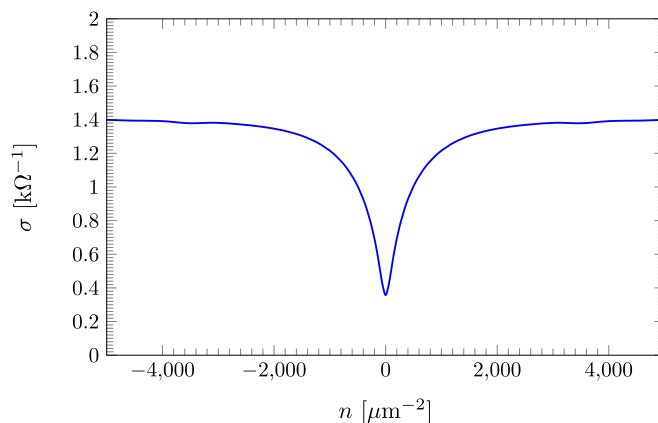


FIG. 6. Electrical conductivity as a function of carrier density. The curve was obtained as the solution of the Boltzmann equation with $\alpha = 0.36$ and $4\pi\gamma^2 = 0.5$ at $T = 75$ K.

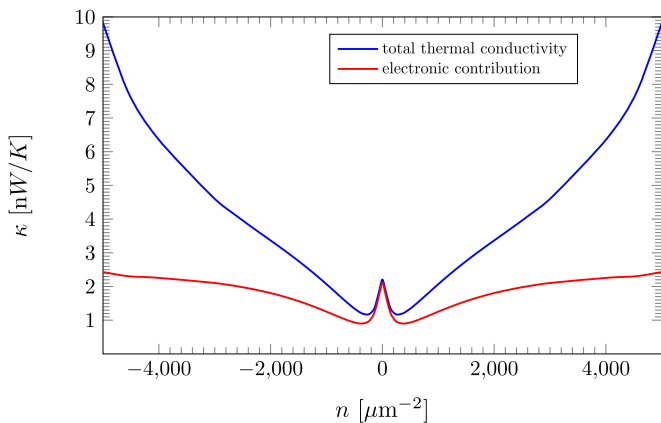


FIG. 7. Thermal conductivity of graphene as a function of the charge carrier density. The curves are calculated using the same set of parameters used in Fig. 6. The blue curve is the full response including the plasmons, while the red curve only shows the electronic contribution. There is a slight plasmon enhancement close to the Dirac point and a massive one with increasing chemical potential.

approximation, which we have done in [40,41] and found that this qualitatively reproduces the full numerical solution presented here.

It is tempting to attribute the growth of the plasmon contribution to its dispersion relation (10), which is $\sqrt{\mu}$ for $\mu/T \gg 1$. However, this is not the sole reason for the increase: Phenomenologically, one expects the thermal conductivity to follow a Drude-type expression $\kappa \propto \int d^2q \omega_p(\vec{q}) \bar{v}_p^2(\vec{q}) (-\frac{\partial b}{\partial \omega_p(\vec{q})}) \tau_p(\vec{q}, \mu)$, where $\tau_p(\vec{q}, \mu)$ is a scattering time that comes from the solution of the Boltzmann equation. If we assume that $\tau_p(\vec{q}, \mu)$ is constant as a function of \vec{q} in the relevant momentum window, we end up with $\kappa \propto \mu^0 \tau_p(0, \mu)$. Consequently, the effect appears to strongly depend on the scattering time, which is born out by an analysis of the scattering integral. To summarize, the main observation is the growing enhancement of the thermal conductivity due to plasmons in the region of $\mu/T > 1$. It is important to note that the relaxation of the plasmons is due to the disorder in the fermionic sector. Momentum that is excited in the plasmon sector through the thermal gradient is

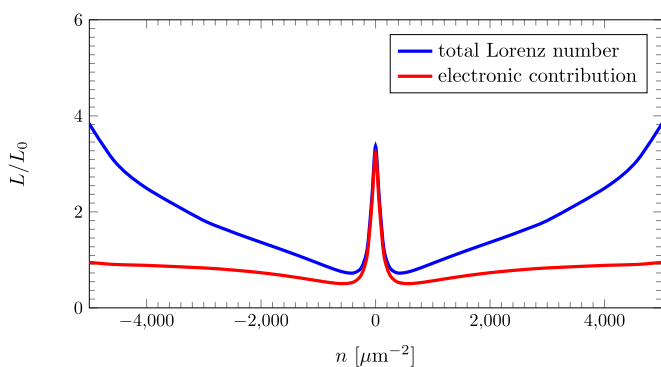


FIG. 8. Wiedemann-Franz ratio as a function of the charge carrier density. We observe two regions with enhancement: the well-known hydrodynamic regime in the vicinity of the Dirac point and at higher doping.

transferred to the fermionic subsystem via inelastic scattering. There it is relaxed from the momentum-conservation-breaking disorder. It is worthwhile noting that around $\mu/T \approx 2$ there is a suppression of the Lorenz ratio below 1. This seems to be a feature that is also encountered in experiments [42].

IV. CONCLUSION AND OUTLOOK

In this work we have analyzed the thermoelectric response of interacting two-dimensional Dirac systems at and away from the Dirac point. We have done so by deriving and solving coupled linearized Boltzmann equations for electrons, holes, and plasmons. At the Dirac point we find a moderate enhancement of the thermal conductivity due to plasmons, compared to the electronic contribution. However, away from the Dirac point, we find a strong enhancement of thermal transport due to plasmons. Compared to a conventional three-dimensional metal, this is made possible by the undamped gapless nature of plasmons which have a square-root dispersion, i.e., $\omega \propto \sqrt{q}$. Consequently, this effect is special to two dimensions and is not expected to exist in three dimensions, in line with very early works [3,4]. The plasmon contribution to the heat conductivity and, connected to that, the violation of the Wiedemann-Franz law increases as we tune into the Fermi liquid regime of a Dirac system. This suggests that the observed effect should also be observable in conventional degenerate two-dimensional metallic systems. While we do not expect a similar effect in three-dimensional metals, we also expect enhancement close to the Dirac point of three-dimensional Dirac and Weyl systems.

The results presented here immediately provoke a series of questions: (i) How can the results be connected to the known results for the disordered two-dimensional Fermi liquid [43]? (ii) How can we model relaxation processes, such as disorder, for plasmons? (iii) Can this effect be observed in experiments? (iv) Can we find a unified hydrodynamic description in which all degrees of freedom enter on equal footing? The answers to some of the above questions are left for future study.

ACKNOWLEDGMENTS

One of the authors (L.F.) acknowledges former collaborations and discussions with S. Sachdev, J. Schmalian, M. Müller, and Jonathan Lux as well as discussions with Andrew Lucas, Rembert Duine, Andrew Mitchell, Henk Stoof, and especially Jonah Waissman. K.P. thanks the Institute for the Promotion of Teaching Science and Technology of Thailand for a Ph.D. fellowship. This work was part of the D-ITP consortium, a program of the Netherlands Organisation for Scientific Research that is funded by the Dutch Ministry of Education, Culture and Science.

APPENDIX A: KELDYSH EQUATIONS

In the following we set up the Keldysh equations for describing transport phenomena in the coupled fermion-plasmon system. The procedure is akin to a system of fermions coupled to phonons where drag effects have to be taken into account. Following standard procedure, we parametrize the fermionic

and bosonic Keldysh components as

$$\begin{aligned} G^K &= G^r \circ F - F \circ G^a, \\ D^K &= D^r \circ B - B \circ D^a, \end{aligned} \quad (\text{A1})$$

where F and B are Hermitian matrices and \circ denotes matrix multiplication in real space and time where $C = A \circ B$ corresponds to $C(\vec{x}_1, t_1, \vec{x}_2, t_2) = \int d\vec{x}' dt' A(\vec{x}_1, t_1, \vec{x}', t') B(\vec{x}', t', \vec{x}_2, t_2)$. Both F and B are, in thermal equilibrium, related to the standard distribution function, where $F = 1 - 2f$ and $B = 1 + 2b$, with f the Fermi-Dirac distribution and b the Bose-Einstein distribution. They obey the kinetic equation according to

$$\begin{aligned} [F, G_0^{-1}]_-^\circ &= \Sigma^K - (\Sigma^r \circ F - F \circ \Sigma^a), \\ [B, D_0^{-1}]_-^\circ &= e^2[\Pi^K - (\Pi^r \circ B - B \circ \Pi^a)], \end{aligned} \quad (\text{A2})$$

where the left-hand sides are commutators involving the bare Green's functions G_0 of the Dirac fermions and D_0 of the plasmons and the right-hand sides are the so-called collision integral. We assume that $e^2\Pi$ is the self-energy of the bosons, whereas Σ is the self-energy of the fermions which we leave unspecified for the moment. We are now going through a series of approximations which will eventually lead us to the Boltzmann equation. We start with a gradient expansion

$$\begin{aligned} [F, G_0^{-1}]_-^\star &= [\Sigma^K - (\Sigma^r \star F - F \star \Sigma^a)], \\ [B, D_0^{-1}]_-^\star &= e^2[\Pi^K - (\Pi^r \star B - B \star \Pi^a)], \end{aligned} \quad (\text{A3})$$

where we have introduced the Moyal product. It has to be interpreted in the following way: There are center-of-mass coordinates $X = (x_1 + x_2)/2$ and $\tilde{T} = (t_1 + t_2)/2$ as well as relative coordinates $x = x_1 - x_2$ and $t = t_1 - t_2$ (note that we introduce the denotation \tilde{T} here to later distinguish it from the temperature T). Furthermore, we perform a Fourier transformation with respect to the relative coordinates, leading to \vec{k} and ω . The Moyal product then reads

$$C(X, \tilde{T}, \vec{k}, \omega) = A(X, \tilde{T}, \vec{k}, \omega) \star B(X, \tilde{T}, \vec{k}, \omega), \quad (\text{A4})$$

with

$$\star = \exp \left[\frac{i}{2} \left(\overleftarrow{\partial}_{\vec{x}} \overrightarrow{\partial}_{\vec{k}} - \overleftarrow{\partial}_{\tilde{T}} \overrightarrow{\partial}_{\omega} - \overleftarrow{\partial}_{\vec{k}} \overrightarrow{\partial}_{\vec{x}} + \overleftarrow{\partial}_{\omega} \overrightarrow{\partial}_{\tilde{T}} \right) \right]. \quad (\text{A5})$$

We perform a leading-order expansion of both the left- and right-hand sides of Eq. (A3),

$$\begin{aligned} i(\partial_{\vec{x}} F \partial_{\vec{k}} \bar{G}^{-1} - \partial_{\vec{k}} F \partial_{\vec{x}} \bar{G}^{-1} - \partial_{\tilde{T}} F \partial_{\omega} \bar{G}^{-1} + \partial_{\omega} F \partial_{\tilde{T}} \bar{G}^{-1}) \\ = \Sigma^K - F(\Sigma^r - \Sigma^a), \end{aligned}$$

$$\begin{aligned} i(\partial_{\vec{x}} B \partial_{\vec{k}} \bar{D}^{-1} - \partial_{\vec{k}} B \partial_{\vec{x}} \bar{D}^{-1} - \partial_{\tilde{T}} B \partial_{\omega} \bar{D}^{-1} + \partial_{\omega} B \partial_{\tilde{T}} \bar{D}^{-1}) \\ = e^2 \Pi^K - e^2 B(\Pi^r - \Pi^a), \end{aligned} \quad (\text{A6})$$

where $\bar{G}^{-1} = G_0^{-1} - \text{Re}\Sigma^r$ and $\bar{D}^{-1} = D_0^{-1} - e^2 \text{Re}\Pi^r$.

These two coupled equations constitute the basis of all further investigations. The next step towards the Boltzmann equation is to replace the functions $F = 1 - 2f$ and $B = 1 + 2b$ with the respective distribution functions leading to

$$\begin{aligned} i2(\partial_{\vec{k}} f \partial_{\vec{x}} G_0^{-1} - \partial_{\vec{x}} f \partial_{\vec{k}} G_0^{-1} + \partial_{\tilde{T}} f \partial_{\omega} G_0^{-1} - \partial_{\omega} f \partial_{\tilde{T}} G_0^{-1}) \\ = \Sigma^K - (1 - 2f)(\Sigma^r - \Sigma^a), \\ i2(\partial_{\vec{x}} b \partial_{\vec{k}} D_0^{-1} - \partial_{\vec{k}} b \partial_{\vec{x}} D_0^{-1} - \partial_{\tilde{T}} b \partial_{\omega} D_0^{-1} + \partial_{\omega} b \partial_{\tilde{T}} D_0^{-1}) \\ = e^2 \Pi^K - e^2(1 + 2b)(\Pi^r - \Pi^a). \end{aligned} \quad (\text{A7})$$

In this paper we concentrate on heat and charge transport. For the left-hand sides of the kinetic equations this implies

$$\begin{aligned} \partial_{\vec{k}} f \partial_{\vec{x}} G_0^{-1} - \partial_{\vec{x}} f \partial_{\vec{k}} G_0^{-1} + \partial_{\tilde{T}} f \partial_{\omega} G_0^{-1} - \partial_{\omega} f \partial_{\tilde{T}} G_0^{-1} \\ = e\vec{E} \partial_{\vec{k}} f - v_F \vec{\sigma} \partial_{\vec{x}} f = e\vec{E} \partial_{\vec{k}} f - v_F \vec{\sigma} \cdot \partial_{\vec{x}} T \partial_T f, \\ \partial_{\vec{x}} b \partial_{\vec{k}} D_0^{-1} - \partial_{\vec{k}} b \partial_{\vec{x}} D_0^{-1} - \partial_{\tilde{T}} b \partial_{\omega} D_0^{-1} + \partial_{\omega} b \partial_{\tilde{T}} D_0^{-1} \\ = 2\epsilon_0 \epsilon_r \frac{\vec{k}}{|\vec{k}|} \partial_{\vec{x}} b = 2\epsilon_0 \epsilon_r \frac{\vec{k}}{|\vec{k}|} \cdot \partial_{\vec{x}} T \partial_T b, \end{aligned} \quad (\text{A8})$$

where T is the temperature. The next step to convert this into a Boltzmann-type equation is to perform the quasiparticle approximation. This is achieved by integrating over the spectral function. To that end we solve the Dyson equation to access the retarded Green's functions G^r and D^r . For G^r it suffices to state that the electrons of holes of graphene are well defined and we thus work with G_0^r , thereby disregarding corrections to infinitely-long-lived quasiparticles. For the plasmons, we use

$$D^r(\vec{q}, \omega) \approx \frac{1}{2\epsilon_0 \epsilon_r} \frac{\omega^2}{q} \frac{1}{(\omega + i0^+)^2 - \omega_p(\vec{q})^2} \quad (\text{A9})$$

with the plasmon dispersion

$$\omega_p(\vec{q}) \approx \sqrt{\alpha \frac{N}{2} k_B T v_F q \ln \left[2 + 2 \cosh \left(\frac{\mu}{k_B T} \right) \right]}, \quad (\text{A10})$$

as derived in the main text.

APPENDIX B: SOURCES OF RELAXATION

The self-energy of the Dirac fermion consists of two parts: One is due to interactions with the plasmons and the other one, due to scattering from impurities, to lowest order, is approximated as

$$\begin{aligned} \Sigma^r(\omega, \vec{k}) - \Sigma^a(\omega, \vec{k}) &= -2e^2 \int \frac{d\nu}{2\pi} \int \frac{d^2q}{(2\pi)^2} [\text{Im}G^r(\omega + \nu, \vec{k} + \vec{q}) D^K(-\nu, -\vec{q}) + G^K(\omega + \nu, \vec{k} + \vec{q}) \text{Im}D^r(-\nu, -\vec{q})] \\ &\quad + \frac{\gamma_0^2}{2} \int \frac{d^2q}{(2\pi)^2} \hat{f}(-\vec{q}) [G^r(\omega, \vec{k} + \vec{q}) - G^a(\omega, \vec{k} + \vec{q})], \\ \Sigma^K(\omega, \vec{k}) &= ie^2 \int \frac{d\nu}{2\pi} \int \frac{d^2q}{(2\pi)^2} [G^K(\omega + \nu, \vec{k} + \vec{q}) D^K(-\nu, -\vec{q}) - 4 \text{Im}G^r(\omega + \nu, \vec{k} + \vec{q}) \text{Im}D^r(-\nu, -\vec{q})] \end{aligned}$$

$$+ \frac{\gamma_0^2}{2} \int \frac{d^2q}{(2\pi)^2} \hat{f}(-\vec{q}) G^K(\omega, \vec{k} + \vec{q}), \quad (\text{B1})$$

where the first line in both cases accounts for scattering of plasmons whereas the second line accounts for disorder scattering. For the plasmons we have

$$\begin{aligned} \Pi^r(\omega, \vec{k}) - \Pi^a(\omega, \vec{k}) &= N \int \frac{d\nu}{2\pi} \int \frac{d^2q}{(2\pi)^2} \text{tr}[\text{Im}G^r(\omega + \nu, \vec{k} + \vec{q}) G^K(\nu, \vec{q}) - G^K(\omega + \nu, \vec{k} + \vec{q}) \text{Im}G^r(\nu, \vec{q})], \\ \Pi^K(\omega, \vec{k}) &= -\frac{i}{2} N \int \frac{d\nu}{2\pi} \int \frac{d^2q}{(2\pi)^2} \text{tr}[G^K(\omega + \nu, \vec{k} + \vec{q}) G^K(\nu, \vec{q}) + 4 \text{Im}G^r(\omega + \nu, \vec{k} + \vec{q}) \text{Im}G^r(\nu, \vec{q})]. \end{aligned} \quad (\text{B2})$$

APPENDIX C: QUASIPARTICLE BASIS

In order to arrive at the final Boltzmann equation we have to project the kinetic equations into the quasiparticle basis. This is straightforward for the plasmons; for the fermions we need a momentum-dependent rotation. To that end we consider the retarded part of the noninteracting fermionic Green's function

$$(G^r)^{-1}(\omega, \vec{k}) = (\omega + \mu)\mathbb{1} - v_F k_x \sigma_x - v_F k_y \sigma_y. \quad (\text{C1})$$

In order to project this onto the quasiparticle basis we need to diagonalize the Green's function (or inverse Green's function). The corresponding unitary transformation reads

$$\begin{aligned} U_{\vec{k}}^{-1} &= \frac{1}{\sqrt{2}k} \begin{pmatrix} k_x - ik_y & -k_x + ik_y \\ k & k \end{pmatrix}, \\ U_{\vec{k}} &= \frac{1}{\sqrt{2}k} \begin{pmatrix} k_x + ik_y & k \\ -k_x - ik_y & k \end{pmatrix}, \end{aligned} \quad (\text{C2})$$

with

$$\begin{aligned} (g^r)^{-1}(\omega, \vec{k}) &= U_{\vec{k}} (G^r)^{-1}(\omega, \vec{k}) U_{\vec{k}}^{-1} \\ &= (\omega + \mu)\mathbb{1} + v_F k \sigma_z. \end{aligned} \quad (\text{C3})$$

APPENDIX D: COUPLED BOLTZMANN EQUATIONS

After having derived the Keldysh equations and specified the collision integral, the last missing pieces towards the Boltzmann equation are a projection into the quasiparticle basis followed by an integration over the spectral functions. To that end we need the retarded part of the Dyson equation. For the plasmons, as discussed before, this reads

$$\begin{aligned} (D^r)^{-1}(\omega, \vec{k}) &= (D_0^r)^{-1}(\omega, \vec{k}) - e^2 \Pi^r(\omega, \vec{k}) \\ &\approx \frac{2\epsilon_0 \epsilon_r k}{\omega^2} [\omega^2 - \omega_p^2(\vec{k})], \end{aligned} \quad (\text{D1})$$

whereas for the fermions we resort to the unperturbed propagator. We furthermore define the form factors

$$\begin{aligned} M_{\vec{q}, \vec{k}+\vec{q}}^{\lambda\lambda'} &= (U_{\vec{q}} U_{\vec{k}+\vec{q}}^{-1})_{\lambda\lambda'} = \frac{1}{2} \left(1 + \lambda\lambda' \frac{Q(K^* + Q^*)}{q|\vec{k} + \vec{q}|} \right), \\ T_{\vec{q}, \vec{k}+\vec{q}}^{\lambda\lambda'} &= M_{\vec{q}, \vec{k}+\vec{q}}^{\lambda\lambda'} M_{\vec{k}+\vec{q}, \vec{q}}^{\lambda'\lambda} = \frac{1}{4} \left| \left(1 + \lambda\lambda' \frac{Q(K^* + Q^*)}{q|\vec{k} + \vec{q}|} \right) \right|^2. \end{aligned} \quad (\text{D2})$$

The poles of the Green's function determine the dispersion $\epsilon_\lambda(\vec{k}) = \lambda v_F k$. This allows us to write the coupled Boltzmann equations as

$$\begin{aligned} &e\vec{E} \partial_{\vec{k}} f_\lambda(\vec{k}) \delta_{\lambda\bar{\lambda}} - v_F (\hat{k} \sigma_z - \hat{k} \times \hat{z} \sigma_y)_{\lambda\bar{\lambda}} \vec{\nabla} T \partial_T f_\lambda(\vec{k}) \\ &= 4\pi v_F \alpha \int \frac{d^2q}{(2\pi)^2} \sum_{\lambda'=\pm} M_{\vec{k}, \vec{k}+\vec{q}}^{\lambda\lambda'} M_{\vec{k}+\vec{q}, \vec{k}}^{\lambda'\lambda} [\delta(\epsilon_{\lambda'}(\vec{k} + \vec{q}) - \epsilon_\lambda(\vec{k}) + \omega_p(\vec{q})) + \delta(\epsilon_{\lambda'}(\vec{k} + \vec{q}) - \epsilon_\lambda(\vec{k}) - \omega_p(\vec{q}))] \\ &\times \frac{\epsilon_{\lambda'}(\vec{k} + \vec{q}) - \epsilon_\lambda(\vec{k})}{q} \{f_\lambda(\vec{k}) [1 - f_{\lambda'}(\vec{k} + \vec{q})] - b_{\epsilon_\lambda(\vec{k}) - \epsilon_{\lambda'}(\vec{k} + \vec{q})}(\vec{q}) [f_{\lambda'}(\vec{k} + \vec{q}) - f_\lambda(\vec{k})]\} \\ &+ \frac{\gamma_0^2}{2\pi} \int \frac{d^2q}{(2\pi)^2} \hat{f}(-\vec{q}) T_{\vec{k}, \vec{k}+\vec{q}}^{\lambda\lambda} \delta_{\lambda\lambda'} \delta(\epsilon_\lambda(\vec{k}) - \epsilon_\lambda(\vec{k} + \vec{q})) [f_\lambda(\vec{k}) - f_\lambda(\vec{k} + \vec{q})] \\ &\frac{\vec{k}}{k^2} \vec{\nabla} T \omega_p(\vec{k}) [\partial_T b_{\omega_p(\vec{k})}(\vec{k}) - \partial_T b_{-\omega_p(\vec{k})}(\vec{k})] \\ &= 4N\pi v_F \alpha \sum_{\lambda, \lambda'=\pm} \int \frac{d^2q}{(2\pi)^2} M_{\vec{q}, \vec{k}+\vec{q}}^{\lambda\lambda'} M_{\vec{k}+\vec{q}, \vec{q}}^{\lambda'\lambda} [\delta(\epsilon_{\lambda'}(\vec{k} + \vec{q}) - \epsilon_\lambda(\vec{q}) + \omega_p(\vec{k})) + \delta(\epsilon_{\lambda'}(\vec{k} + \vec{q}) - \epsilon_\lambda(\vec{q}) - \omega_p(\vec{k}))] \\ &\times \frac{\epsilon_{\lambda'}(\vec{k} + \vec{q}) - \epsilon_\lambda(\vec{q})}{k} \{f_{\lambda'}(\vec{k} + \vec{q}) [f_\lambda(\vec{q}) - 1] - b_{\epsilon_{\lambda'}(\vec{k} + \vec{q}) - \epsilon_\lambda(\vec{q})}(\vec{k}) [f_{\lambda'}(\vec{k} + \vec{q}) - f_\lambda(\vec{q})]\}. \end{aligned} \quad (\text{D3})$$

In equilibrium we have

$$f_\lambda^0(\vec{k}) = \frac{1}{e^{(\epsilon_\lambda(\vec{k}) - \mu)/T} + 1}, \quad b_\omega^0(\vec{k}) = \frac{1}{e^{\omega/T} - 1}. \quad (\text{D4})$$

The second term on the left-hand side of the first line corresponds to the Berry phase term which comes from the adiabatic projection into the quasiparticle basis. The fourth term is the thermal analog of the zitterbewegung. These terms makes no regular contribution in our calculation and are subsequently omitted.

APPENDIX E: LINEARIZED BOLTZMANN EQUATION

We then proceed to linearize the Boltzmann equations. To that end we introduce the parametrization

$$\begin{aligned} f_\lambda(\vec{k}) &= f_\lambda^0(\vec{k}) + \frac{1}{T^2} f_\lambda^0(\vec{k}) [1 - f_\lambda^0(\vec{k})] \lambda v_F \hat{k} [e\vec{E} \chi_\lambda^E(k) + \vec{\nabla} T \chi_\lambda^T(k)], \\ b_{\omega_p(\vec{k})}(\vec{k}) &= b_{\omega_p(\vec{k})}^0(\vec{k}) + \frac{1}{T^2} b_{\omega_p(\vec{k})}^0(\vec{k}) [1 + b_{\omega_p(\vec{k})}^0(\vec{k})] v_F \hat{k} [e\vec{E} \phi^E(k) + \vec{\nabla} T \phi^T(k)]. \end{aligned} \quad (\text{E1})$$

Using the linearization and neglecting the Berry phase as well as the off-diagonal contribution, we obtain

$$\begin{aligned} & -\lambda e \frac{v_F}{T} \hat{k} \cdot \vec{E} f_\lambda^0(\vec{k}) (1 - f_\lambda^0(\vec{k})) - \lambda \frac{v_F}{T} \hat{k} \vec{\nabla} T \frac{\epsilon_\lambda(\vec{k}) - \mu}{T} f_\lambda^0(\vec{k}) [1 - f_\lambda^0(\vec{k})] \\ &= \alpha \frac{4\pi v_F^2}{T^2} \int \frac{d^2 q}{(2\pi)^2} \sum_{\lambda'=\pm} M_{\vec{k}, \vec{k}+\vec{q}}^{\lambda\lambda'} M_{\vec{k}+\vec{q}, \vec{k}}^{\lambda'\lambda} [\delta(\epsilon_{\lambda'}(\vec{k} + \vec{q}) - \epsilon_\lambda(\vec{k}) + \omega_p(\vec{q})) + \delta(\epsilon_{\lambda'}(\vec{k} + \vec{q}) - \epsilon_\lambda(\vec{k}) - \omega_p(\vec{q}))] \\ & \quad \times \frac{\epsilon_{\lambda'}(\vec{k} + \vec{q}) - \epsilon_\lambda(\vec{k})}{q} f_\lambda^0(\vec{k}) [1 - f_\lambda^0(\vec{k})] [1 - f_{\lambda'}^0(\vec{k} + \vec{q}) + b_{\epsilon_\lambda(\vec{k}) - \epsilon_{\lambda'}(\vec{k} + \vec{q})}^0(\vec{q})] \\ & \quad \times \left[e\vec{E} \left(\lambda \frac{\vec{k}}{k} \chi_\lambda^E - \lambda' \frac{\vec{k} + \vec{q}}{|\vec{k} + \vec{q}|} \chi_{\lambda'}^E(|\vec{k} + \vec{q}|) + \frac{\vec{q}}{q} \phi^E(q) \right) + \vec{\nabla} T \left(\lambda \frac{\vec{k}}{k} \chi_\lambda^T - \lambda' \frac{\vec{k} + \vec{q}}{|\vec{k} + \vec{q}|} \chi_{\lambda'}^T(|\vec{k} + \vec{q}|) + \frac{\vec{q}}{q} \phi^T(q) \right) \right] \\ & \quad + \frac{\gamma_0^2 v_F}{2\pi T^2} \int \frac{d^2 q}{(2\pi)^2} \hat{f}(-\vec{q}) T_{\vec{k}, \vec{k}+\vec{q}}^{\lambda\lambda} \delta_{\lambda\lambda'} \delta(\epsilon_\lambda(\vec{k}) - \epsilon_\lambda(\vec{k} + \vec{q})) f_\lambda^0(\vec{k}) [1 - f_\lambda^0(\vec{k})] \\ & \quad \times \left[e\vec{E} \left(\lambda \frac{\vec{k}}{k} \chi_\lambda^E - \lambda' \frac{\vec{k} + \vec{q}}{|\vec{k} + \vec{q}|} \chi_{\lambda'}^E(|\vec{k} + \vec{q}|) \right) + \vec{\nabla} T \left(\lambda \frac{\vec{k}}{k} \chi_\lambda^T - \lambda' \frac{\vec{k} + \vec{q}}{|\vec{k} + \vec{q}|} \chi_{\lambda'}^T(|\vec{k} + \vec{q}|) \right) \right], \\ & \frac{\vec{k}}{k^2} \vec{\nabla} T \frac{\omega_p^2(\vec{k})}{T^2} b_{\omega_p(\vec{k})}^0(\vec{k}) [1 + b_{\omega_p(\vec{k})}^0(\vec{k})] \\ &= \alpha 4N\pi \frac{v_F^2}{T^2} \sum_{\lambda, \lambda'=\pm} \int \frac{d^2 q}{(2\pi)^2} M_{\vec{q}, \vec{k}+\vec{q}}^{\lambda\lambda'} M_{\vec{k}+\vec{q}, \vec{q}}^{\lambda'\lambda} [\delta(\epsilon_{\lambda'}(\vec{k} + \vec{q}) - \epsilon_\lambda(\vec{q}) + \omega_p(\vec{k})) + \delta(\epsilon_{\lambda'}(\vec{k} + \vec{q}) - \epsilon_\lambda(\vec{q}) - \omega_p(\vec{k}))] \\ & \quad \times \frac{\epsilon_{\lambda'}(\vec{k} + \vec{q}) - \epsilon_\lambda(\vec{q})}{k} f_\lambda^0(\vec{q}) [1 - f_\lambda^0(\vec{q})] [f_{\lambda'}^0(\vec{k} + \vec{q}) + b_{\epsilon_{\lambda'}(\vec{k} + \vec{q}) - \epsilon_\lambda(\vec{q})}^0(\vec{k})] \\ & \quad \times \left[e\vec{E} \left(\lambda \frac{\vec{q}}{q} \chi_\lambda^E - \lambda' \frac{\vec{k} + \vec{q}}{|\vec{k} + \vec{q}|} \chi_{\lambda'}^E(|\vec{k} + \vec{q}|) + \frac{\vec{k}}{k} \phi^E(k) \right) + \vec{\nabla} T \left(\lambda \frac{\vec{q}}{q} \chi_\lambda^T - \lambda' \frac{\vec{k} + \vec{q}}{|\vec{k} + \vec{q}|} \chi_{\lambda'}^T(|\vec{k} + \vec{q}|) + \frac{\vec{k}}{k} \phi^T(k) \right) \right]. \end{aligned} \quad (\text{E2})$$

Our ansatz for the deviation from equilibrium reads

$$\begin{aligned} \chi_\lambda^E(k) &= a_{0,\lambda}^E + a_{1,\lambda}^E k = a_{0,\lambda}^E |E, 0, \lambda\rangle + a_{1,\lambda}^E |E, 1, \lambda\rangle, \\ \chi_\lambda^T(k) &= a_{0,\lambda}^T + a_{1,\lambda}^T k = a_{0,\lambda}^T |T, 0, \lambda\rangle + a_{1,\lambda}^T |T, 1, \lambda\rangle, \\ \phi^E(k) &= b_0^E + b_1^E k = b_0^E |E, 0\rangle + b_1^E |E, 1\rangle, \\ \phi^T(k) &= b_0^T + b_1^T k = b_0^T |T, 0\rangle + b_1^T |T, 1\rangle. \end{aligned} \quad (\text{E3})$$

One can rewrite the Boltzmann equations in a more compact form as

$$\begin{aligned} |Df, E, \lambda\rangle + |Df, T, \lambda\rangle &= |I_{\text{coll}}, E\rangle + |I_{\text{coll}}, T\rangle, \\ |Db, T\rangle &= |\tilde{I}_{\text{coll}}, E\rangle + |\tilde{I}_{\text{coll}}, T\rangle. \end{aligned} \quad (\text{E4})$$

To determine the expansion coefficients in Eq. (E4) we define a scalar product according to

$$\langle f | g \rangle = \int \frac{d^2 k}{(2\pi)^2} f(k) \frac{\vec{k}}{k} g(\vec{k}). \quad (\text{E5})$$

This allows us to convert the linearized Boltzmann equations into a linear algebra problem which we can solve for $a_{0,1,\lambda}^{E,T}$ and $b_{0,1}^{E,T}$.

- [1] P. Drude, Zur elektronentheorie der metalle, *Ann. Phys. (Leipzig)* **306**, 566 (1900).
- [2] N. W. Ashcroft and N. D. Mermin, *Solid State Physics* (Saunders, Philadelphia, 1976).
- [3] D. Pines and D. Bohm, A collective description of electron interactions: II. Collective vs individual particle aspects of the interactions, *Phys. Rev.* **85**, 338 (1952).
- [4] D. Bohm and D. Pines, A collective description of electron interactions: III. Coulomb interactions in a degenerate electron gas, *Phys. Rev.* **92**, 609 (1953).
- [5] L. Landau, Kinetic equation for the case of Coulomb interaction, *Phys. Z. Sowjetunion* **10**, 154 (1936).
- [6] D. Pines, A collective description of electron interactions: IV. Electron interaction in metals, *Phys. Rev.* **92**, 626 (1953).
- [7] A. A. Vlasov, The vibrational properties of an electron gas, *Sov. Phys. Usp.* **10**, 721 (1968).
- [8] J. Ziman, *Electrons and Phonons* (Oxford University Press, Oxford, 2000).
- [9] R. Franz and G. Wiedemann, Ueber die wärme-leitungs-fähigkeit der metalle, *Ann. Phys. Chem.* **165**, 497 (1853).
- [10] R. Gurzhi, Minimum of resistance in impurity-free conductors, *J. Exp. Theor. Phys. (U.S.S.R.)* **44**, 771 (1963).
- [11] A. A. Abrikosov and I. M. Khalatnikov, The theory of a Fermi liquid (the properties of liquid ^3He at low temperatures), *Rep. Prog. Phys.* **22**, 329 (1959).
- [12] M. J. M. de Jong and L. W. Molenkamp, Hydrodynamic electron flow in high-mobility wires, *Phys. Rev. B* **51**, 13389 (1995).
- [13] A. Levchenko and J. Schmalian, Transport properties of strongly coupled electron-phonon liquids, *Ann. Phys. (NY)* **419**, 168218 (2020).
- [14] X. Huang and A. Lucas, Electron-phonon hydrodynamics, *Phys. Rev. B* **103**, 155128 (2021).
- [15] N. P. Armitage, E. J. Mele, and A. Vishwanath, Weyl and Dirac semimetals in three-dimensional solids, *Rev. Mod. Phys.* **90**, 015001 (2018).
- [16] K. S. Novoselov, A. K. Geim, S. V. Morozov, D. Jiang, M. I. Katsnelson, I. V. Grigorieva, S. V. Dubonos, and A. A. Firsov, Two-dimensional gas of massless Dirac fermions in graphene, *Nature (London)* **438**, 197 (2005).
- [17] A. H. Castro Neto, F. Guinea, N. M. R. Peres, K. S. Novoselov, and A. K. Geim, The electronic properties of graphene, *Rev. Mod. Phys.* **81**, 109 (2009).
- [18] D. E. Sheehy and J. Schmalian, Quantum Critical Scaling in Graphene, *Phys. Rev. Lett.* **99**, 226803 (2007).
- [19] S. A. Hartnoll, P. K. Kovtun, M. Müller, and S. Sachdev, Theory of the Nernst effect near quantum phase transitions in condensed matter and in dyonic black holes, *Phys. Rev. B* **76**, 144502 (2007).
- [20] A. B. Kashuba, Conductivity of defectless graphene, *Phys. Rev. B* **78**, 085415 (2008).
- [21] L. Fritz, J. Schmalian, M. Müller, and S. Sachdev, Quantum critical transport in clean graphene, *Phys. Rev. B* **78**, 085416 (2008).
- [22] M. Müller, L. Fritz, and S. Sachdev, Quantum-critical relativistic magnetotransport in graphene, *Phys. Rev. B* **78**, 115406 (2008).
- [23] H.-Y. Xie and M. S. Foster, Transport coefficients of graphene: Interplay of impurity scattering, Coulomb interaction, and optical phonons, *Phys. Rev. B* **93**, 195103 (2016).
- [24] M. Schütt, P. M. Ostrovsky, I. V. Gornyi, and A. D. Mirlin, Coulomb interaction in graphene: Relaxation rates and transport, *Phys. Rev. B* **83**, 155441 (2011).
- [25] B. N. Narozhny, Electronic hydrodynamics in graphene, *Ann. Phys. (NY)* **411**, 167979 (2019).
- [26] B. Wunsch, T. Stauber, F. Sols, and F. Guinea, Dynamical polarization of graphene at finite doping, *New J. Phys.* **8**, 318 (2006).
- [27] S. Das Sarma and Q. Li, Intrinsic plasmons in two-dimensional dirac materials, *Phys. Rev. B* **87**, 235418 (2013).
- [28] D. C. Elias, R. V. Gorbachev, A. S. Mayorov, S. V. Morozov, A. A. Zhukov, P. Blake, L. A. Ponomarenko, I. V. Grigorieva, K. S. Novoselov, F. Guinea, and A. K. Geim, Dirac cones reshaped by interaction effects in suspended graphene, *Nat. Phys.* **7**, 701 (2011).
- [29] J. Crossno, J. K. Shi, K. Wang, X. Liu, A. Harzheim, A. Lucas, S. Sachdev, P. Kim, T. Taniguchi, K. Watanabe, T. A. Ohki, and K. C. Fong, Observation of the Dirac fluid and the breakdown of the Wiedemann-Franz law in graphene, *Science* **351**, 1058 (2016).
- [30] A. Lucas, J. Crossno, K. C. Fong, P. Kim, and S. Sachdev, Transport in inhomogeneous quantum critical fluids and in the Dirac fluid in graphene, *Phys. Rev. B* **93**, 075426 (2016).
- [31] D. A. Bandurin, I. Torre, R. Krishna Kumar, M. Ben Shalom, A. Tomadin, A. Principi, G. H. Auton, E. Khestanova, K. S. Novoselov, I. V. Grigorieva, L. A. Ponomarenko, A. K. Geim, and M. Polini, Negative local resistance caused by viscous electron backflow in graphene, *Science* **351**, 1055 (2016).
- [32] D. A. Bandurin, A. V. Shytov, L. S. Levitov, R. K. Kumar, A. I. Berdyugin, M. Ben Shalom, I. V. Grigorieva, A. K. Geim, and G. Falkovich, Fluidity onset in graphene, *Nat. Commun.* **9**, 4533 (2018).
- [33] P. Gallagher, C.-S. Yang, T. Lyu, F. Tian, R. Kou, H. Zhang, K. Watanabe, T. Taniguchi, and F. Wang, Quantum-critical conductivity of the Dirac fluid in graphene, *Science* **364**, 158 (2019).
- [34] G. Mahan, *Many-Particle Physics*, 3rd ed. (Springer, New York, 2000).
- [35] M. Müller and S. Sachdev, Collective cyclotron motion of the relativistic plasma in graphene, *Phys. Rev. B* **78**, 115419 (2008).
- [36] D. F. DuBois and M. G. Kivelson, Electron correlational effects on plasmon damping and ultraviolet absorption in metals, *Phys. Rev.* **186**, 409 (1969).
- [37] E. G. Mishchenko, M. Y. Reizer, and L. I. Glazman, Plasmon attenuation and optical conductivity of a two-dimensional electron gas, *Phys. Rev. B* **69**, 195302 (2004).
- [38] A. Kamenev, *Field Theory of Non-Equilibrium Systems* (Cambridge University Press, Cambridge, 2011).
- [39] L. Fritz, Quantum critical transport at a semimetal-to-insulator transition on the honeycomb lattice, *Phys. Rev. B* **83**, 035125 (2011).
- [40] K. Pongsangangan, T. Ludwig, H. T. C. Stoof, and L. Fritz, Hydrodynamics of charged two-dimensional Dirac systems. I. Thermoelectric transport, *Phys. Rev. B* **106**, 205126 (2022).
- [41] K. Pongsangangan, T. Ludwig, H. T. C. Stoof, and L. Fritz, Hydrodynamics of charged Dirac electrons in two dimensions. II. Role of collective modes, *Phys. Rev. B* **106**, 205127 (2022).
- [42] J. Weissman (private communication).
- [43] G. Catelani and I. Aleiner, Interaction corrections to thermal transport coefficients in disordered metals: The quantum kinetic equation approach, *J. Exp. Theor. Phys.* **100**, 331 (2005).